

**MINISTRY OF EDUCATION AND TRAINING
NHA TRANG UNIVERSITY**

PHAM VAN THU

**BUCKLING STUDY OF THREE-PHASE COMPOSITE
PLATE USED IN SHIPBUILDING FABRICATION**

SUMMARY OF THE PHD THESIS

KHANH HOA-2020

**MINISTRY OF EDUCATION AND TRAINING
NHA TRANG UNIVERSITY**

PHAM VAN THU

**BUCKLING STUDY OF THREE-PHASE COMPOSITE
PLATE USED IN SHIPBUILDING FABRICATION**

Major: Mechanical Dynamics Engineering

Major code: 9520116

SUMMARY OF THE PHD THESIS

SUPERVISOR:

- 1. PROF.SC.D NGUYEN DINH DUC**
- 2. PHD. NGUYEN VAN DAT**

KHANH HOA – 2020

The work has been completed at Nha Trang University

Science instructor: **1. PROF.SC.D NGUYEN DINH DUC**
2. PHD. NGUYEN VAN DAT

Reviewer 1:

Reviewer 2:

Reviewer 3:

**The thesis is protected at the Thesis Evaluation Board, held at Nha
Trang University at....., on.....**

This thesis can be found at: The National Library

The Library of Nha Trang University

Thesis title: "Buckling Study of three-phase composite plate used in shipbuilding fabrication"

Major: Mechanical Dynamics Engineering

Major code: 9520116

PhD Student: **Pham Van Thu**

Course: 2013

Supervisor: 1. **Prof. Sc.D Nguyen Dinh Duc**

2. **PhD. Nguyen Van Dat**

Education Institution: Nha Trang University.

Key findings:

1. The equation and the static buckling calculation of the three-phase polymer orthotropic composite plates have been established, which are subject to one-direction compression, simultaneous compression in both directions and shear load. Determined the critical force value of the three-phase polymer orthotropic composite plate in the case that all edges of the plates are single supported and clamped. At the same time, the impact of factors such as the load, parameters and material composition ratio, geometric dimensions on the static buckling of three-phase polymer composite plates was assessed.
2. The equation and the dynamic buckling calculation of three-phase polymer composite panels with hydrodynamic load have been established in two cases that all edges of the plates are single supported and clamped. Assessed the influence of factors such as: layout to layers, geometric dimensions, ship speed, initial shape imperfection, material composition on dynamic buckling of three-phase polymer composite panels. Investigated the effect of geometric dimensions, the ratio of particles and fibers composition to the vibration frequency of a three-phase composite panel. Determined the critical force value, critical speed of three-phase composite panel under hydrodynamic load.
3. Constructed method of buckling calculation of hydrofoil lift wings by analytical method based on design criteria of hydrofoil structure. Determined the permissible stable bending stress, permissible bending moment of the wing. From that, determined the geometric dimension of the wings that met the design criteria of hydrofoil structure.
4. During the implementation of the thesis, successfully tested three-phase polymer composite materials (polymer matrix, fibers, particles) and experimentally determined the elastic modules of the material. The results showed that three-phase composite has superior advantages compared to two-phase composite with only substrate and fiber. Since then, this result is suggested using to study static and dynamic buckling of three-phase composite structures in reality.



GS.TSKH. Nguyễn Đình Đức

PhD Student



Pham Van Thu

INTRODUCTION

1. Reason for topic selection

In actual shipbuilding of composite materials, for waterproofing, increase in surface hardness against hull erosion and hard-to-burn materials, domestic shipyards have been added to the polymer matrix TiO₂ particles or Firegard B flame retardant. Thus, the actual composite material will be three phases: polymer matrix, fibers and particles. However, they have only been tested and no research has been done on them.

Currently, domestic shipyards are in need of researching and manufacturing hydrofoil boat made of composite materials. Lifting wings are components made from large and complex loading plates. Their instability will lead to a decrease in lift, and thus obscure the main role of the wings (instability of the entire ship).

Therefore, the topic "*Buckling study of three-phase composite plate used in shipbuilding fabrication*" of the thesis is an urgent issue of scientific and practical significance..

2. Study objectives

- Determine the static buckling of the three-phase composite plates under the impact of mechanical loads.
- Determine the dynamic buckling of three-phase composite panel under the impact of hydrodynamic load.

3. Study subject and scope

Three-phase composite plates and panels (polymer matrix based on TiO₂ particles and fiberglass) are the ship shell and hydrofoil cover, respectively. The scope of the study is static (of three-phase orthotropic plates in three cases: two-directional compression; one-directional compression and shear load) and dynamic buckling.

4. Study Methodology

- The thesis use thin plate theory, Bubnov-Galerkin and Runge-Kutta methods to set up and solve mechanical equations with analytic solutions. The calculation results are compared with the results obtained by other authors and with the Ansys software commonly used today to check the accuracy of the thesis.
- Making samples, experimenting to determine the three-phase composite material coefficients at the Laboratory of Institute of Ship Research and Development.

5. Scientific and practical significance of the topic

The formulas are explicitly expressed through the material and geometric properties of the plate, from which we can change such parameters to select the appropriate plate for technical requirement satisfaction. The study results will provide the scientific basis for the behavior of three-phase composite materials and the basic equations for stability study of the three-phase plate are practical significant problems in shipbuilding industry.

6. Thesis structure

The thesis includes: introduction, four chapters, conclusion and recommendations, list of the author's study works related to the thesis content, references and appendices.

CHAPTER I: OVERVIEW OF FIELD OF STUDY

Presenting research results domestically and internationally on three-phase composite, static and dynamic stabilization of composite plates. From the published works, practical requirements and open directions mentioned, the fellow focuses on studying:

- Determining the elastic modulus of a three-phase composite subject to the parameters and ratio of component materials.
- Studying the static buckling of the three-phase orthotropic plates (shell, deck, etc.) subjected two-directional compression, one-directional compression and shear load (referred to as mechanical load).
- Studying the dynamic buckling of three-phase composite panel for hydrofoil cover.

CHAPTER II: DETERMINATION OF ELASTIC MODULUS OF THREE-PHASE COMPOSITE

There are two main methods of determining elastic modulus of materials: experiment and analysis. The advantage of the experimental method is precisely determining the elastic modulus of the composite, but three-phase composite is a multi-component material, the experiment does not reflect the influence of the component material phases on mechanical properties of composite.

2.1. Determine elastic coefficients of three-phase composite

2.1.1. Three-phase composite model of fibers and reinforced particles

It is assumed that each layer of the plate is a unidirectional fiber-reinforced three-phase composite, then the three-phase polymer composite model is shown in Figure 2.1. The problem for three-phase composite materials is how to calculate the elastic coefficients of the material, and at the same time express it through mechanical-physical parameters and geometric distribution of the component materials.

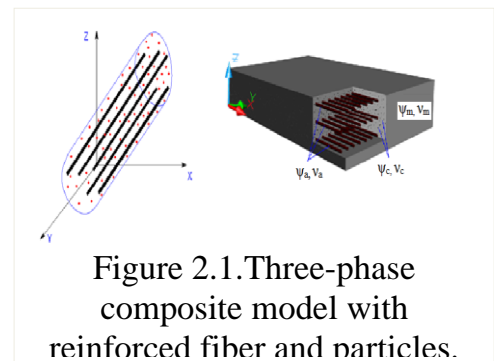


Figure 2.1. Three-phase composite model with reinforced fiber and particles.

2.1.2. The calculation model for determination of the elastic coefficients of three-phase composite materials

Three-phase composite has been proposed to research and solve scientific problems posed by the methods in [13,97], that is solved step by step in a two-phase model from the perspective described by the formula:

$$1D_m = O_m + 1D \quad (2.1)$$

The first step: considering two-phase composite including: the initial matrix and the fill particles, such composite is considered homogeneous, isotropic and has 2 elastic coefficients. The elastic coefficients of the O_m composite are now called the assumed composite.

The second step: determining the elastic coefficients of the composite between the assumed matrix and the reinforced fibers.

2.1.3. Determine the elastic coefficients of the material

It is assumed the components of the composite (matrix, fiber, particle) are homogeneous and

isotropic, then we will denote E_m, G_m, ν_m, ψ_m ; E_a, G_a, ν_a, ψ_a ; E_c, G_c, ν_c, ψ_c are the elastic modulus, poisson coefficient and component proportion (by volume) of matrix, fiber and particles. According to [120], elastic modulus of assumed composite is as follows:

$$\bar{G} = G_m \frac{1 - \psi_c(7 - 5\nu_m)H}{1 + \psi_c(8 - 10\nu_m)H} \quad \bar{K} = K_m \frac{1 + 4\psi_c G_m L(3K_m)^{-1}}{1 - 4\psi_c G_m L(3K_m)^{-1}} \quad (2.2-2.3)$$

$$\text{Vói: } L = \frac{K_c - K_m}{K_c + \frac{4G_m}{3}}; \quad H = \frac{G_m / G_c - 1}{8 - 10\nu_m + (7 - 5\nu_m) \frac{G_m}{G_c}} \quad (2.4)$$

$G_i = \frac{E_i}{2(1+\nu_i)}$ vói $i = m, a, c$; $\bar{E}, \bar{\nu}$ is calculated from \bar{K}, \bar{G} as follows:

$$\bar{E} = \frac{9\bar{K}\bar{G}}{3\bar{K} + \bar{G}} \quad \bar{\nu} = \frac{3\bar{K} - 2\bar{G}}{6\bar{K} - 2\bar{G}} \quad (2.5)$$

\bar{G}, \bar{K} : Sliding elastic module and block module of the assumed matrix

We have selected the unidirectional fiber-reinforced three-phase composite elastic modulus according to the formulas of G.S Vanin [119] with 6 independent coefficients as follows:

$$E_{11} = \psi_a E_a + (1 - \psi_a) \bar{E} + \frac{8\bar{G}\psi_a(1 - \psi_a)(\nu_a - \bar{\nu})}{2 - \psi_a + \bar{\chi}\psi_a + (1 - \psi_a)(\chi_a - 1) \frac{\bar{G}}{G_a}}$$

$$E_{22} = \left\{ \frac{\nu_{21}^2}{E_{11}} + \frac{1}{8\bar{G}} \left[\frac{2(1 - \psi_a)(\bar{\chi} - 1) + (\chi_a - 1)(\bar{\chi} - 1 + 2\psi_a) \frac{\bar{G}}{G_a}}{2 - \psi_a + \bar{\chi}\psi_a + (1 - \psi_a)(\chi_a - 1) \frac{\bar{G}}{G_a}} + 2 \frac{\bar{\chi}(1 - \psi_a) + (1 + \psi_a \bar{\chi}) \frac{\bar{G}}{G_a}}{\bar{\chi} + \psi_a + (1 - \psi_a) \frac{\bar{G}}{G_a}} \right] \right\}^{-1}$$

$$G_{12} = \bar{G} \frac{1 + \psi_a + (1 - \psi_a) \frac{\bar{G}}{G_a}}{1 - \psi_a + (1 + \psi_a) \frac{\bar{G}}{G_a}}; \quad G_{23} = \bar{G} \frac{\bar{\chi} + \psi_a + (1 - \psi_a) \frac{\bar{G}}{G_a}}{(1 - \psi_a)\bar{\chi} + (1 + \bar{\chi}\psi_a) \frac{\bar{G}}{G_a}};$$

$$\nu_{23} = -\frac{E_{22}\nu_{21}^2}{E_{11}} + \frac{E_{22}}{8\bar{G}} \left[2 \frac{(1 - \psi_a)\bar{\chi} + (1 + \psi_a \bar{\chi}) \frac{\bar{G}}{G_a}}{\bar{\chi} + \psi_a + (1 - \psi_a) \frac{\bar{G}}{G_a}} - \frac{2(1 - \psi_a)(\bar{\chi} - 1) + (\chi_a - 1)(\bar{\chi} - 1 + 2\psi_a) \frac{\bar{G}}{G_a}}{2 - \psi_a + \bar{\chi}\psi_a + (1 - \psi_a)(\chi_a - 1) \frac{\bar{G}}{G_a}} \right]$$

$$\nu_{21} = \bar{\nu} - \frac{(\bar{\chi} + 1)(\bar{\nu} - \nu_a)\psi_a}{2 - \psi_a + \bar{\chi}\psi_a + (1 - \psi_a)(\chi_a - 1) \frac{\bar{G}}{G_a}} \quad (2.6)$$

With $\bar{\chi} = 3 - 4\bar{\nu}$; $\chi_a = 3 - 4\nu_a$; $\nu_{12} = \frac{E_{11}}{E_{22}} \nu_{21}$

2.2. Numeric calculations and experiment

2.2.1. Numeric calculations

Considering the influence of fibers and particles on the physical and mechanical properties of the three-phase composite according to the above algorithm, the three-phase composite materials with the characteristics in Table 2.1 are considered:

Table 2.1: Specifications of composite component materials

AKA polyester matrix (Viet Nam)	$E_m = 1.43$	$\nu_m=0.345$
Fiberglass (Korea)	$E_a = 22.0$	$\nu_a=0.24$
TiO ₂ particles (Australia)	$E_c = 5.58$	$\nu_c=0.20$

Replace the values in Table 2.1 into the formulas (2.2) ÷ (2.6) to determine the elastic coefficients of three-phase composite materials as shown in figures 2.2÷ 2.4.

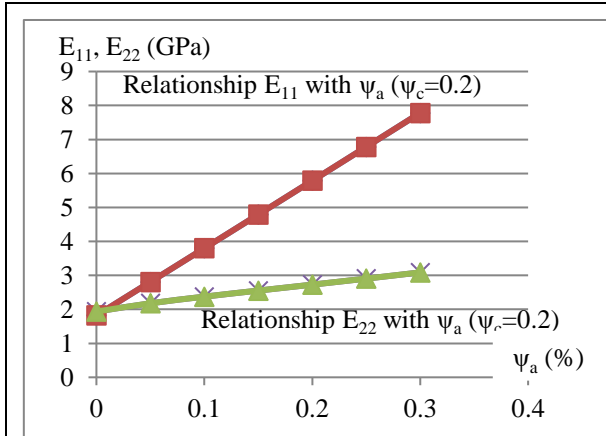


Figure 2.2. Graph of relationship between E_{11} , E_{22} and ψ_a

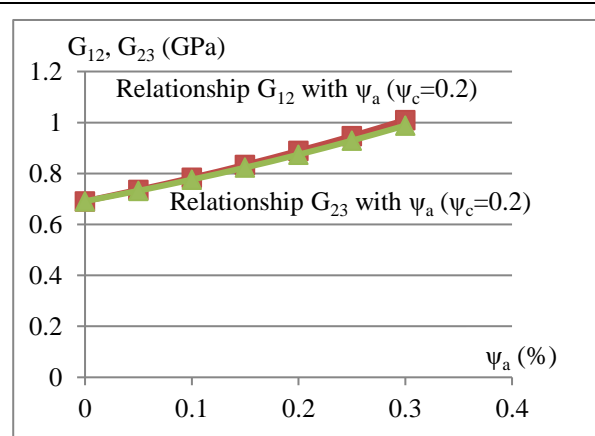


Figure 2.3. Graph of relationship between G_{12} , G_{23} and ψ_a

2.2.2. Experiment

Experiment aims to verify the theoretical results just found. Component materials for specimen manufacturing are as shown in Table 2.1. 4 combinations of specifications for specimen manufacturing: 1) 20% TiO₂ + 15% Fibers; 2) 20% TiO₂ + 20% Fibers; 3) 20% TiO₂ + 25% Fibers; 4) 20% TiO₂ + 30% Fibers.

Tension specimen is processed according to BS EN ISO 527-4: 1997 with b×h = 10×3 ÷ 4mm as shown in Figure 2.5.

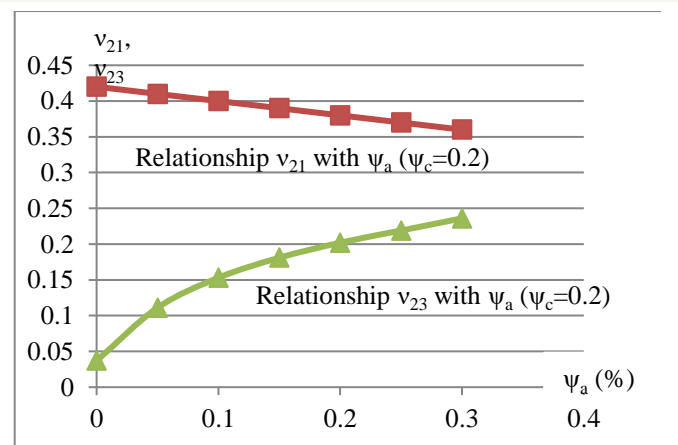


Figure 2.4. Graph of relations between ν_{21} , ν_{23} and ψ_a



Figure 2.5. Prepare test specimens



Figure 2.6. HOUNSFEILDH50K-S tester

The tester is a HOUNSFEILDH 50K-S, a maximum load capacity of 50000N, force and elongation accuracy of $\pm 0.5\%$ and $\pm 0.05\%$ respectively as shown in Figure 2.6.

The theoretical calculation results according to the formula (2.2) - (2.6) compared with the experiment [18] are presented in Table 2.3.

Table 2.3: Comparison between theory and experiment in the presence of 20% TiO₂.

Three-phase composite		Result (MPa)	
		E ₁₁	E ₂₂
20%TiO ₂ + 15%W800 + 65% resin AKA	Experiment	5064.9	2680.3
	Theory	4791.1	2553.2
	Error	5.71%	4.98%
20%TiO ₂ + 20%W800 + 60% resin AKA	Experiment	5620.1	2951.7
	Theory	5785.9	2728.2
	Error	2.87%	8.19%
20%TiO ₂ + 25%W800 + 55% resin AKA	Experiment	6570.2	3106.1
	Theory	6782.9	2905.4
	Error	3.14%	6.91%
20%TiO ₂ + 30%W800 + 50% resin AKA	Experiment	6258.4	2663.4
	Theory	7782.2	3088.4
	Error	19.58%	13.76%

In addition, there are theoretical and experimental results with resin 9509 as follows:

Table 2.4: Parameters of composite component materials.

Polyester resin 9509 (Malaysia)	E _m = 1.50	v _m =0.34
Fiberglass E (China)	E _a = 25.0	v _a =0.24
TiO ₂ particles (Australia)	E _c = 5.58	v _c =0.20

Table 2.5: Comparison between theory and experiment in the presence of 5% TiO₂.

Three-phase composite		Result (MPa)	
		E ₁₁	E ₂₂
5%TiO ₂ + 25%W800 + 70% resin 9509	Experiment	7905.6	2497.2
	Theory	7367.5	2629.0
	Error	7.30%	5.01%
5%TiO ₂ + 30%W800 + 65% resin 9509	Experiment	9104.7	2695.4
	Theory	8529.0	2805.7
	Error	6.75%	3.93%
5%TiO ₂ + 40%W800 + 55% resin 9509	Experiment	11389.2	3353.0
	Theory	10858.1	3190.3
	Error	4.89%	5.10%

Tables 2.3 and 2.5 show that: - In the actual construction of composite materials, the good ratio between reinforcement and matrix is about 45% ÷ 55%, combining research results showing a good fit between the results theoretically and experimentally.

- The effect of fibers on the mechanical properties of the material is better than that of TiO₂ particles.

The obtained results allow us to be confident when using the formula for calculating elastic coefficients of materials and algorithms mentioned above.

2.3. Chapter 2 conclusion.

The thesis has solved: determinate elastic modules for three-phase composite,

depending on the parameters and the ratio of component materials. The advantage of this method is that it is possible to calculate and predict the values of the elastic module, which is the basis of the new material optimization design.

CHAPTER III: STATIC BUCKLING OF THREE-PHASE COMPOSITE PLATES IMPACTED BY MECHANICAL LOAD

In fact shipbuilding composite materials, when added to the polymer matrix of fire-retardant additive particles, or TiO₂ particles to increase surface hardness and prevent hull erosion, the sheet's mechanical properties will change [18]. Therefore, upon the considerable change in mechanical properties of composite plates, load bearing capacity and stability of the structure will be impacted.

In this section, explanation on static stability of three-phase composite plates under the impact of mechanical load will be shown for the specific case where the third phase is TiO₂ particle; it is also the general method upon replacing this phase with another filler.

3.1. . Stability classification and stability criteria

3.1.1. Stability classification

- Type I buckling is case where the critical load is achieved at bifurcation point.
- Type II buckling is the case where the critical load is achieved at the extreme point of the load deflection curve.

3.1.2. Stability criteria

To study static stability of the elastic system, criteria: motion, statics and energy can be used....The thesis uses static criterion to study the static stability problem.

3.2. Fundamental equation of static stability

From documents [20, 25, 26, 70, 71] and design manual [49], and their practical application widely used; in addition, most of the composite materials used in the industry of shipbuilding in Vietnam are currently of orthotropic configuration, the fellow selects orthotropic plates as the basis for building static buckling equation for three-phase composite plates.

The equation of buckling of orthotropic plates is:

$$\begin{aligned} D_{11} \frac{\partial^4 w_0}{\partial x^4} + 2(D_{12} + 2D_{66}) \frac{\partial^4 w_0}{\partial x^2 \partial y^2} + D_{22} \frac{\partial^4 w_0}{\partial y^4} \\ = N_x \frac{\partial^2 w_0}{\partial x^2} + 2N_{xy} \frac{\partial^2 w_0}{\partial x \partial y} + N_y \frac{\partial^2 w_0}{\partial y^2} + q \end{aligned} \quad (3.23)$$

3.2.1. Buckling of three-phase orthotropic plates subjected two-directional compression

According to (3.23), the governing equation for the buckling of the orthotropic rectangular plate simply supported on four sides and subject to uniform compression with the corresponding forces of $N_x = -N_0$ and $N_y = -\beta N_0$, without horizontal load becomes:

$$D_{11} \frac{\partial^4 w_0}{\partial x^4} + 2(D_{12} + 2D_{66}) \frac{\partial^4 w_0}{\partial x^2 \partial y^2} + D_{22} \frac{\partial^4 w_0}{\partial y^4} = -N_0 \frac{\partial^2 w_0}{\partial x^2} - \beta N_0 \frac{\partial^2 w_0}{\partial y^2} \quad (3.24)$$

Boundary conditions: - $x = 0$ and $x = a$: $w_0 = 0$; $M_x = -D_{11} \frac{\partial^2 w_0}{\partial x^2} - D_{12} \frac{\partial^2 w_0}{\partial y^2} = 0$
 - When $y = 0$ and $y = b$: $w_0 = 0$; $M_y = -D_{12} \frac{\partial^2 w_0}{\partial x^2} - D_{22} \frac{\partial^2 w_0}{\partial y^2} = 0$

Put $w_0(x, y) = A_{mn} \sin \frac{m\pi x}{a} \sin \frac{n\pi y}{b}$ into (3.24) for the solution N_0 depending on $\psi_a, \psi_c, a/b$ and e , respectively the volume ratio of fiber, particle and geometric dimensions of plates:

$$N_0 = N_{(\psi_a, \psi_c, a/b, e)} = \frac{\pi^2 \left[(P_1 + 1)P_2 m^4 + 2 \left(\nu_{21} P_2 + \frac{e^3}{6} G_{12} \right) m^2 n^2 R^2 + \left(\frac{E_{22}}{E_{11}} - P_1 \right) P_2 n^4 R^4 \right]}{\alpha^2 (m^2 + \beta n^2 R^2)} \quad (3.27)$$

Where: $P_1 = (R_Q - 1)\alpha = \left(\frac{E_{22}}{E_{11}} - 1 \right) \alpha$ và $P_2 = \frac{e^3}{12} \frac{E_{11}}{1 - \nu_{12}^2 R_Q} = \frac{e^3}{12} \frac{E_{11}}{1 - \nu_{12}^2 \frac{E_{22}}{E_{11}}}$

Equation (3.27) is the equation with the variables: $\psi_a, \psi_c, a/b$ and e used to study the buckling of three-phase orthotropic plates subjected simultaneous two-directional compression.

The critical force corresponds to the values of m and n making N_0 smallest. With $m=n=1$, the expression (3.27) becomes:

$$N_{th}(1,1) = \frac{\pi^2 \left[(P_1 + 1)P_2 + 2 \left(\nu_{21} P_2 + \frac{e^3}{6} G_{12} \right) R^2 + \left(\frac{E_{22}}{E_{11}} - P_1 \right) P_2 R^4 \right]}{\alpha^2 (1 + \beta R^2)} \quad (3.28)$$

3.2.2. Buckling of three-phase orthotropic plates subjected one-directional compression

Considering one orthotropic rectangular plate, simply supported on four sides (boundary conditions are as in section 3.2.1) and compressed in x direction, then $\beta=0$ and (3.27) become:

$$N_0 = N_{(\psi_a, \psi_c, a/b, e)} = \frac{\pi^2 \left[(P_1 + 1)P_2 m^4 + 2 \left(\nu_{21} P_2 + \frac{e^3}{6} G_{12} \right) m^2 n^2 R^2 + \left(\frac{E_{22}}{E_{11}} - P_1 \right) P_2 n^4 R^4 \right]}{m^2 \alpha^2} \quad (3.29)$$

The equation (3.29) is the equation with the variables: $\psi_a, \psi_c, a/b$ and e used to study the buckling of three-phase orthotropic plates subjected one-directional compression.

The smallest value of N_0 corresponding to $n = 1$ at $R = [m(m + 1)]^{1/2} \left(\frac{P_1 + 1}{\frac{E_{22}}{E_{11}} - P_1} \right)^{1/4}$ is:

$$N_{th}(m, 1) = \frac{\pi^2 \left[(P_1 + 1)P_2 m^4 + 2 \left(\nu_{21} P_2 + \frac{e^3}{6} G_{12} \right) m^2 R^2 + \left(\frac{E_{22}}{E_{11}} - P_1 \right) P_2 R^4 \right]}{m^2 \alpha^2} \quad (3.30)$$

3.2.3. Buckling of three-phase orthotropic plates subjected shear load

Considering one orthotropic plate of axb dimensions, clamped on four sides, subjected uniform shear load by N_{xy} force.

Boundary conditions:- When $x = 0$ and $x = a$: $w_0 = 0$; $\frac{\partial w_0}{\partial x} = 0$
 - When $y = 0$ and $y = b$: $w_0 = 0$; $\frac{\partial w_0}{\partial y} = 0$

Combining [119, 120], [27] and [56, 114], S_{th} critical load of the three-phase polymer composite plate depends on ψ_a , ψ_c , a/b and e as follows:

$$S_{th} = N(\psi_a, \psi_c, \frac{a}{b}, e) = \frac{k_s \pi^2 \sqrt[4]{(P_1 + 1)P_2 \left[\left(\frac{E_{22}}{E_{11}} - P_1 \right) P_2 \right]^3}}{b^2} \quad (3.33)$$

Where: The shear buckling parameter k_s is determined from [68]

$$\theta(\psi_a, \psi_c, e) = \frac{\sqrt{(P_1 + 1)P_2 \left(\frac{E_{22}}{E_{11}} - P_1 \right) P_2}}{\nu_{21} P_2 + \frac{e^3}{6} G_{12}}; \quad B(\psi_a, \psi_c, \frac{a}{b}, e) = \frac{b}{a} \sqrt[4]{\frac{(P_1 + 1)P_2}{\left(\frac{E_{22}}{E_{11}} - P_1 \right) P_2}}$$

The equation (3.33) used to study the buckling of three-phase orthotropic plates subjected shear load.

3.3. Survey of buckling of three-phase composite plates subjected mechanical load

Survey of three-phase composite plates of $a \times b$ dimensions, the order of layers noted $7(90/0) \equiv [90/0/90/0/90/0/90]$ and $7(0/90) \equiv [0/90/0/90/0/90/0]$, plates are composed of the following: AKA matrix: $E_m = 1.43$ GPa, $\nu_m = 0.345$; Fiberglass: $E_a = 22.0$ GPa $\nu_a = 0.24$; TiO_2 particles: $E_c = 5.58$ GPa, $\nu_c = 0.20$

$$(3.34)$$

3.3.1. Buckling of three-phase orthotropic plates subjected two-directional compression

Replace the values (3.34) into the formula (3.28) to have results shown in the following figures:

3.3.1.1. Effect of fiber, particle ratio on critical force of plates subjected two-directional compression:

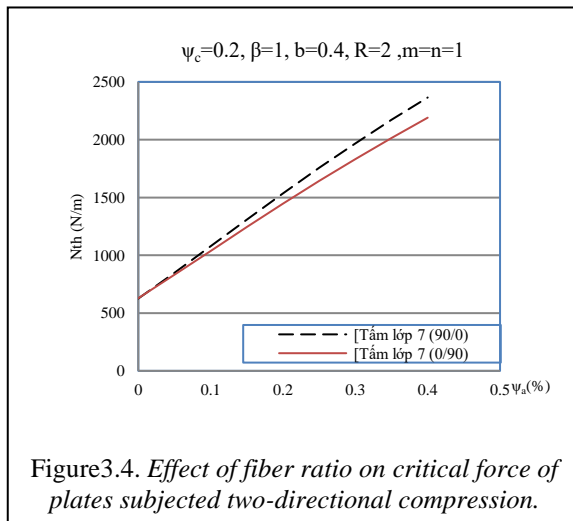


Figure3.4. Effect of fiber ratio on critical force of plates subjected two-directional compression.

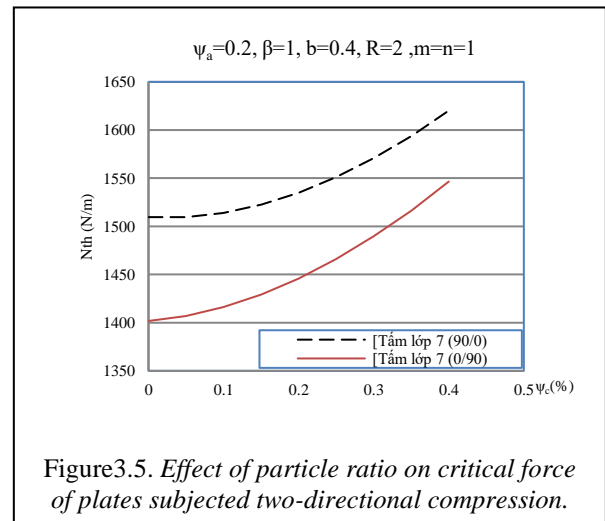
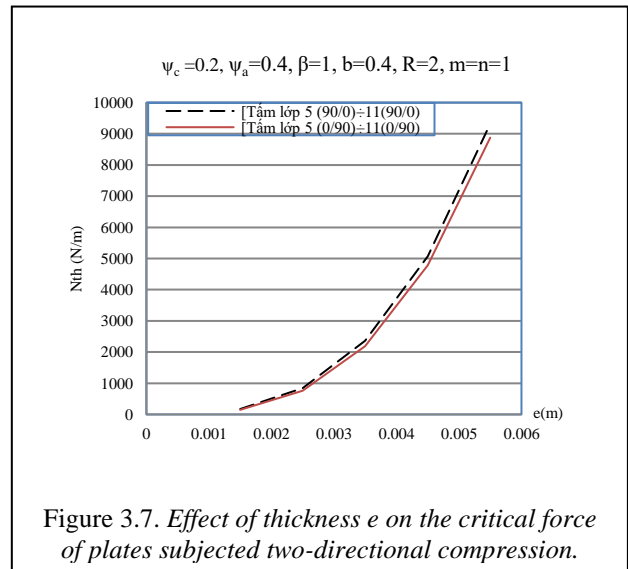
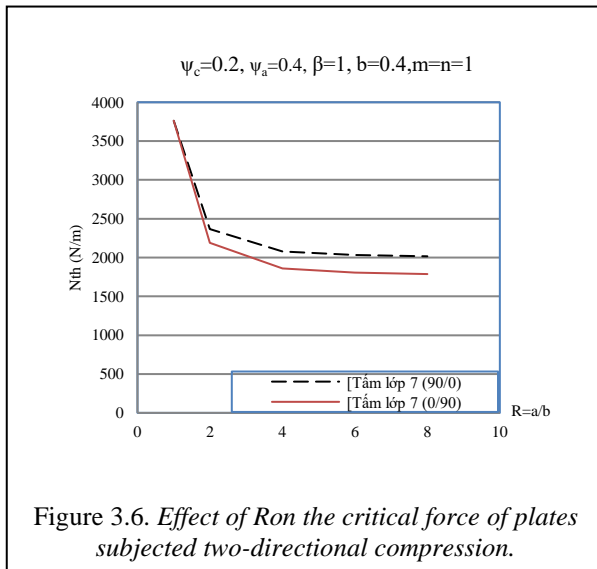


Figure3.5. Effect of particle ratio on critical force of plates subjected two-directional compression.

- When the fiber and particle ratio increase, the two-directional compression resistance of plates goes up. The orthotropic plate has a 25% fiber + 20% particle ratio, which is 12% better stable than the orthotropic plate with 20% fiber + 25% particle.
- Layer placement sequence impacts the buckling of plates; the value between two plates differs from 5÷8% (plate 7(90/0) has better bearing capacity than plate 7(0/90)).

3.3.1.2. Effect of coefficient $R=a/b$, e on the critical force of plates subjected simultaneous two-directional compression.

- Orthotropic plates have an increase in geometric ratio 2 times and replace 5% of fiber with 5% of particles (then the proportion of fiber is 20%), the ability to withstand critical force decreases by 44%. Show that 20% of the fiber is not a reasonable proportion (must be greater than 20%) of the composite plate in force-bearing.
- Orthotropic plates have a ratio of 40% fiber + 20% particle, when the thickness varies from 2.5 ÷ 5.5mm and if replacing 5% fiber with 5% particle, the stability of the plate will decrease by 11 ÷ 12%.

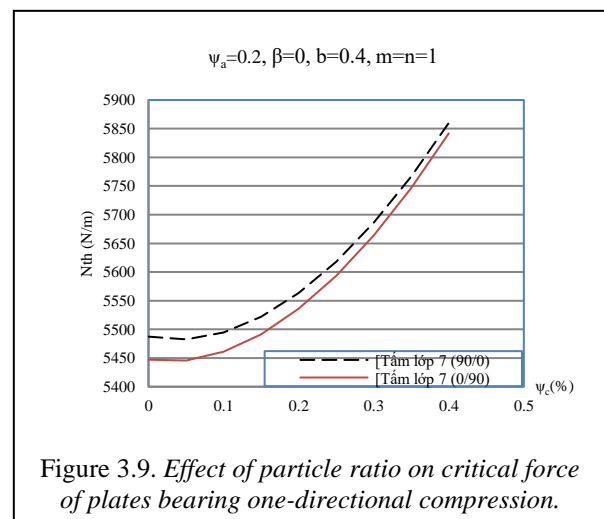
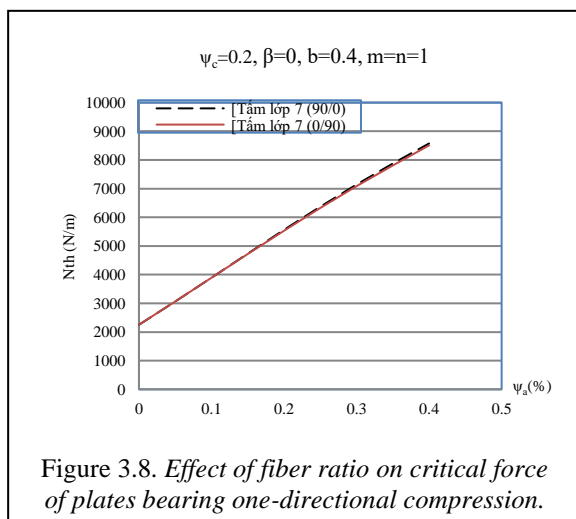


3.3.2. Buckling of three-phase orthotropic plates subjected one-directional compression

Replace the values (3.34) into the formula (3.30) to have results shown in the following figures:

3.3.2.1. Effect of fiber, particle ratio on critical force of plates subjected one-directional compression.

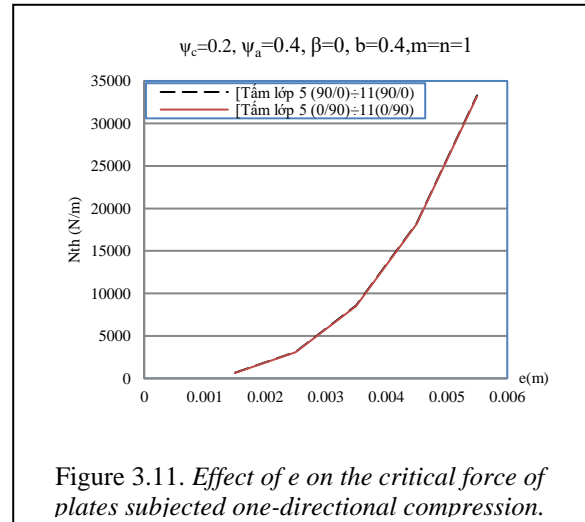
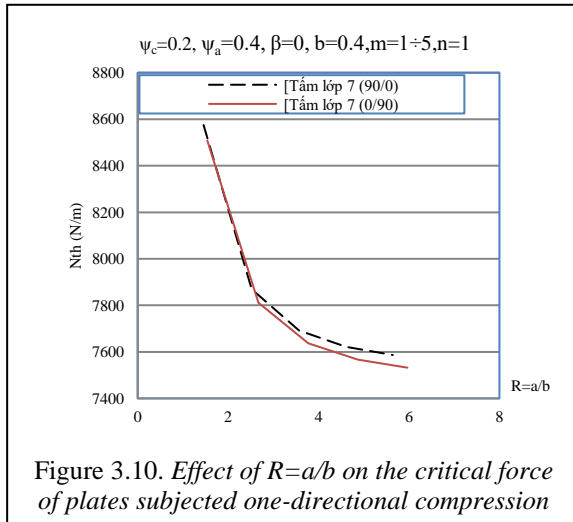
- When the fiber and particle ratio increase, the one-directional compression resistance of plates goes up; the effect of fiber on the plate's buckling is better than particle's.



- Orthotropic plates with a ratio of 25% fiber + 20% particles have a better stability of 13% compared to the orthotropic plate with a ratio of 20% fiber + 25% particles subjected to compression in one direction.

3.3.2.2. Effect of coefficient $R=a/b$, e on the critical force of plates subjected one-directional compression

- Orthotropic plates have an increase in geometric ratio of 2.5 times ($R = 2.5$), stability decreases by 10% when compressing in one direction.



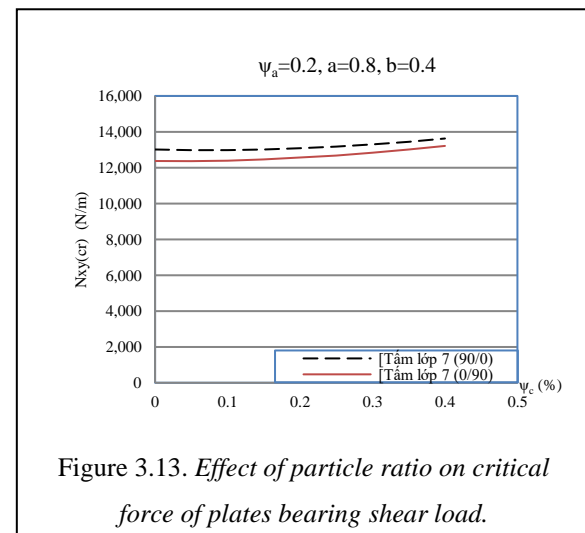
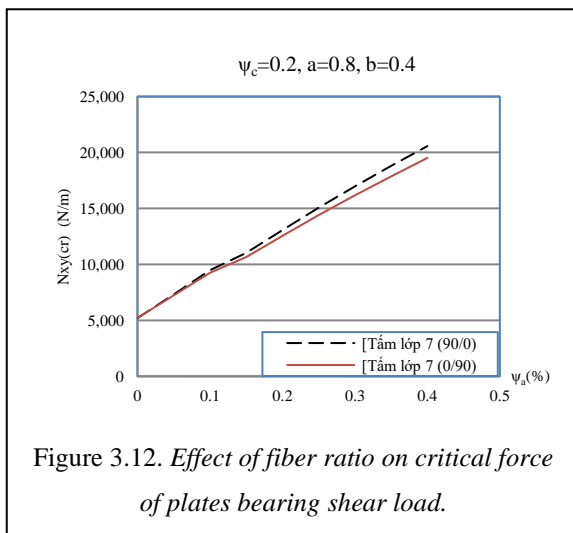
- When the thickness is changed from $2.5 \div 5.5$ mm, if replacing 5% of *fiber* with 5% of *particles* (then the fiber ratio is 20%), the stability of sheet will decrease $8 \div 12\%$. Thus, the geometric ratio plays an important role in bearing force and ensures the stability of the sheet when compressing in one direction.

3.3.3. Buckling of three-phase orthotropic plates subjected shear load

Replace the values (3.34) into the formula (3.33) to have results shown in the following figures:

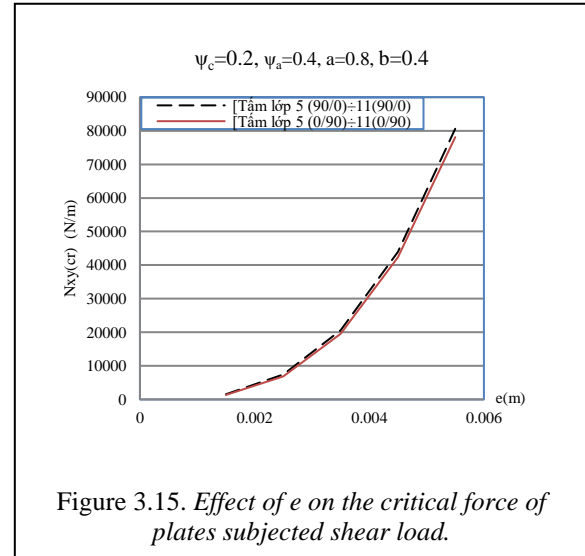
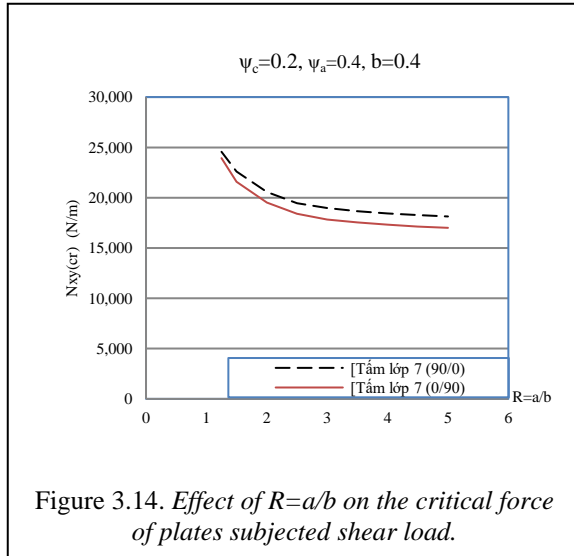
3.3.3.1. Effect of fiber, particle ratio on critical force of plates subjected shear load.

- The shear strength of plates having the component ($\psi_a=0.4, \psi_c=0.2$) is $(1.48 \div 1.51)$ times higher than the shear strength of the component ($\psi_a=0.2, \psi_c=0.4$).



- Orthotropic plates with 25% fiber + 20% particles ratio have better stability 12.6% compared to the orthotropic plate with 20% fiber + 25% particles under shear load. As such, the *fiber* ratio plays an important role in force-bearing and ensures the stability of the sheet under shearing.

3.3.3.2. Effect of $R = a/b$, e on the critical force of plates subjected shear load.



-When the R coefficient increases, the critical force of plates subjected shear load decreases, rapidly at first then slowly. R increases from 1.25 ÷ 2.5 times, S_{th} decreases by 0.77 time.

- Orthotropic plates have an increase in geometric ratio 2 times and replace 5% of fiber with 5% of particles (then the proportion of fiber is 20%), the stability is reduced by 37%.

3.3.4. Comparison of thesis findings with other studies

In two cases: simultaneous compression in two and one directions, the results were similar to those of Leissa [68].

3.4. Chapter 3 conclusion.

- Equations (3.28), (3.30) and (3.33) are established for the buckling analysis of three-phase orthotropic plates subjected mechanical load.

- Buckling of three-phase orthotropic plates bearing mechanical load is surveyed. Effect of material parameter and component ratio of fiber, particle, geometric dimensions of plates, and configure on buckling of plates is also determined.

CHAPTER IV:

DYNAMIC BUCKLING OF THREE-PHASE COMPELITE PANELS

Wing calculation model is shown in Figure 4.1.b. Thus, it can be seen that the most difficult problem is the foil buckling when hardened to the two central struts.

Firstly, to solve the problem, it is necessary to define the permitted limits for the hydrofoil to ensure buckling in the modes when operation. The following are some of the buckling standards to be considered for the object of study.

4.1. Buckling standard

4.1.1. Budiansky-Roth standard

Under the effect of dynamic load, the system's displacement response over time has increasing amplitude, in which the system is not stable in case of sudden increase of amplitude. Values corresponding to the time when the amplitude increases suddenly are called critical values.



Figure 4.1.a. Hydrofoil ship

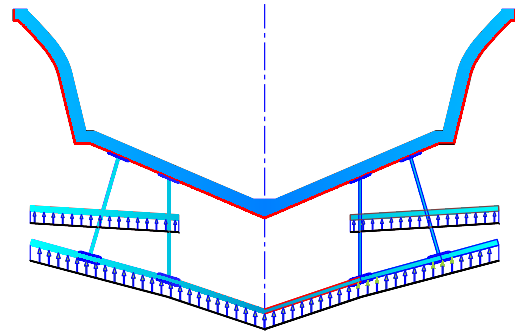


Figure 4.1.b. Arrangement of lifting foils to the hydrofoil ship shell.

4.1.2. Hydrofoil ship structural design standard [81]

4.1.2.1. The method of determining allowable bending buckling stresses and moments

According to [81] allowable bending buckling stress and allowable bending moment of foil and struts is determined.

4.1.2.2. Determination of the hydrofoil size from the buckling standard.

- For aluminum foils.

It is assumed that the hydrofoil is made of aluminum material 5456 with: $\sigma_{ch}=19(\text{Ksi})$ and $E=10300(\text{Ksi})$. The foil of NACA 16-018 with $c=4(\text{ft})$, shell thickness $t=1/2(\text{inches})$ and an unsupported panel width $b=305.3(\text{mm})$ is chosen. Then $b/t=24$, according to [81], the shape and size of the foil are satisfied the allowable bending buckling stress and allowable bending moment as shown in Figure 4.5.

From the dynamic parameters of the foil [140], and according to [48,81,143], the lifting force acting on the foil is determined:

$$L = \frac{1}{2} \rho C_L S V^2 \quad (4.4)$$

The maximum bending moment appears in fixed ends:

$$M_{max} = \frac{w'l^2}{12} \quad (4.5)$$

Replace the values in (4.5): $M_{max} = 155144 < M_{cp} = 206026.5(\text{N.m})$ (Satisfied) (**)

Maximum deflection of foil at position between two clamped edges:

$$f_{max} = \frac{w'l^4}{384EJ_y} \quad (4.6)$$

Replace the values in (4.6) and combine (*): $f_{max}=0.0013 < f_{cp} = \frac{M_{cp}l^2}{32EJ_{y.cp}} = 0.0019 (m)^{(1)}$ (satisfied) (***)

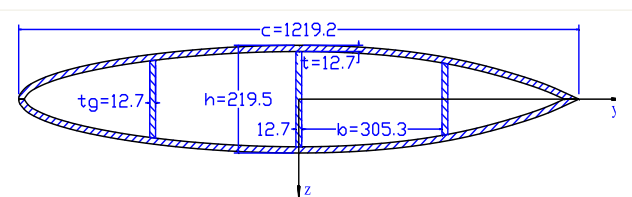


Figure 4.5. Cross section of NACA 16-018 foil satisfies (*)

Maximum bending stress generated on the skin layer of the foil:

$$\sigma_{max} = \frac{M_{max}}{J_y} z \quad (4.7)$$

In which: $z = h/2=0.11(m)$: at the skin layer on the foil;

Replace the values in (4.7): $\sigma_{max} = 79.45 < \sigma_{cr} = 118.04(MPa)$ (satisfied) (***)).

Comment: Combine (), (***) and (****), the foil with cross section as shown in Figure 4.5 satisfies static buckling with distance of two maximum clamped edges of 2 (m).**

- **For composite foils.**

The above-mentioned aluminum foil is changed into composite material according to the following equivalent model:

- The hydrodynamic size and shape (outside) are the same;
- Values such as: The maximum bending moment, the maximum deflection of the foil, the maximum bending stress generated on the skin layer of the foil are within the above-mentioned permitted limits.

These two models are equivalent when the hardness value of the

aluminum foil model is equal to the hardness of the composite foil model, that is: $E_{Al}J_{Al} = E_C J_C$. On the other hand, to ensure strength in all directions, here will take the value of strength and hardness in the direction of 45^0 to calculate [18]. Or the layers of fiber are arranged in the order as shown in Figure (4.9): The quasi-isotropic materials. Gradually adjust the foil size and reinforcement ribs, select a foil with a cross section with inertial moment that suitable with the expected value. From the explanation on the composite foil, the size as shown in Figure 4.10 is equivalent to the aluminum foil.

4.1.2.3. Determination of the allowable deflection from the buckling standard.

Similar 4.1.2.2, it is necessary to collect statistical data on the allowable deflection of NACA 16-018 foil made of aluminum 5456 with $c = 1 \div 7 (ft)$. On the other hand, replace (4.7) into (4.6) we have:

$$f_{cp} = \frac{l^2}{32E} \frac{\sigma_{cr}}{z} \quad (4.8)$$

By the least square method, the curves and regression functions of the functional relationship between f_{cp} and variables c and σ_{cr} can be set.

Table 4.6: Regression equation for the allowable deflection of the foil.

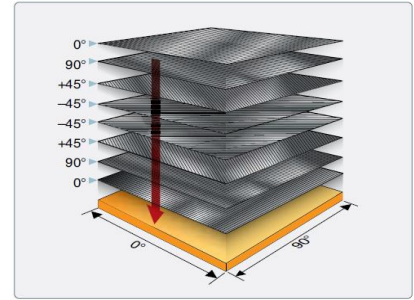


Figure 4.9. The quasi-isotropic materials [139].

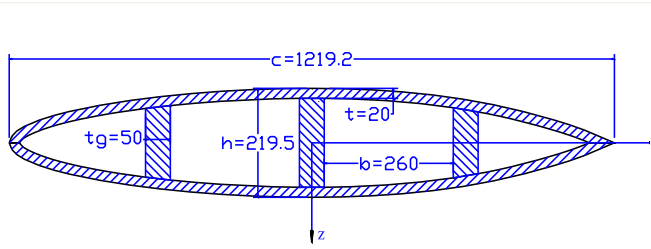


Figure 4.10. Cross section of composite foil is equivalent to aluminum foil.

No	Parameter of foil	Regression functions	
		Equation	Realibility
01	Foil chord length $c = 2(\text{ft})$	$y = 3.208236226 \cdot 10^{-5}x$	$R^2 = 0.999$
02	Foil chord length $c = 3(\text{ft})$	$y = 2.138850140 \cdot 10^{-5}x$	$R^2 = 0.999$
03	Foil chord length $c = 4(\text{ft})$	$y = 1.600151054 \cdot 10^{-5}x$	$R^2 = 0.999$
04	Foil chord length $c = 5(\text{ft})$	$y = 1.283388059 \cdot 10^{-5}x$	$R^2 = 0.999$
05	Foil chord length $c = 6(\text{ft})$	$y = 1.069412075 \cdot 10^{-5}x$	$R^2 = 0.999$
06	Foil chord length $c = 7(\text{ft})$	$y = 9.166389217 \cdot 10^{-6}x$	$R^2 = 0.999$

From the collected data, the regression curves are shown in Figure 4.12:

Comment: - The results show that it is easy to determine the allowable deflection value through the regression function.

- The values obtained in figure 4.12 are the standard for evaluating the buckling of hydrofoil.

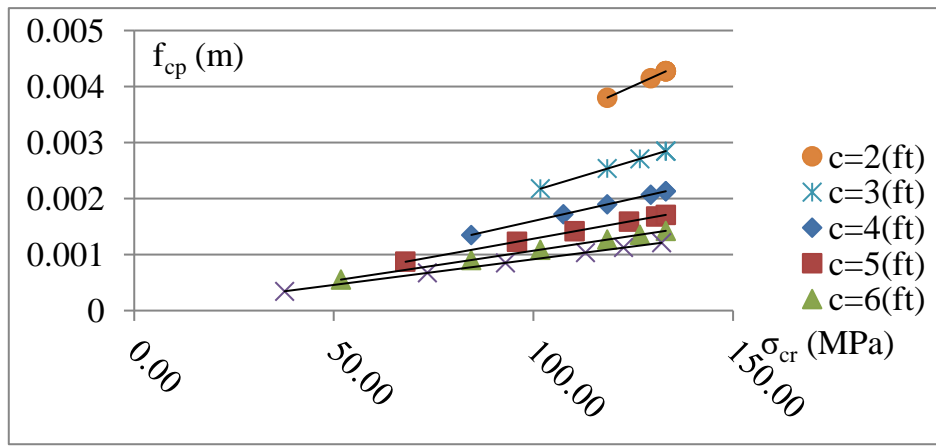


Figure 4.12. Regression curve for allowable deflection of the foil.

- The deflection is proportional to the square of the distance of two struts (the value in Figure 4.12 is built with the distance of two struts $l = 2(\text{m})$).

4.2. Dynamic buckling equation of three-phase composite panel under the impact of hydrodynamic load.

Considering the three-phase composite panel is the shell of the lifting foil sized and subjected to the hydrodynamic load: the lifting force q_1 and the drag q_2 shown in Figure 4.14. The classical shell theory is here used to establish the governing equation and determine the nonlinear response of the composite panel.

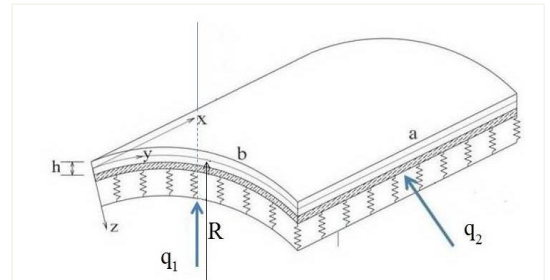


Figure 4.14. Shape and coordinate system of three-phase composite panel on elastic foundation.

The nonlinear equation of motion of the composite panel is based on classical plate theory ([27], [91], [105]), combining the Volmir hypothesis (Volmir 1972)

$u \ll w, v \ll w, \rho_1 \frac{\partial^2 u}{\partial t^2} \rightarrow 0, \rho_1 \frac{\partial^2 v}{\partial t^2} \rightarrow 0$, we have:

$$N_{x,x} + N_{xy,y} = 0, \quad (4.22a)$$

$$N_{xy,x} + N_{y,y} = 0, \quad (4.22b)$$

$$M_{x,xx} + 2M_{xy,xy} + M_{y,yy} + N_x w_{,xx} + 2N_{xy} w_{,xy} + N_y w_{,yy} + q_1 + q_2 - k_1 w + k_2 \nabla^2 w + \frac{N_y}{R} = \rho_1 \frac{\partial^2 w}{\partial t^2} \quad (4.22c)$$

In which: $\rho_1 = \rho h$ with $\rho = 1550$ (kg/m³) is the density of the composite panel and q_1 , q_2 is determined according to the formula (4.4) which coefficients are $C_L = 0.86$ and $C_x = 0.03$ [48, 81, 143].

For imperfect composite panels, equation (4.25) is given into:

$$P_1 f_{,xxxx} + P_2 f_{,yyyy} + P_3 w_{,xxyy} + P_4 w_{,xxxy} + P_5 w_{,xyyy} + P_6 w_{,xxxx} + P_7 w_{,yyyy} + P_8 w_{,xxyy} + P_9 w_{,xxxy} + P_{10} w_{,xyyy} + f_{,xy} (w_{,xx} + w_{,xx}^*) - 2f_{,xy} (w_{,xy} + w_{,xy}^*) + f_{,xx} (w_{,yy} + w_{,yy}^*) + q_1 + q_2 - k_1 w + k_2 \nabla^2 w + \frac{N_y}{R} = \rho_1 \frac{\partial^2 w}{\partial t^2} \quad (4.28)$$

Where: $w^*(x, y)$ is function representing for imperfection of the panel's original shape

4.2.1. In case of all edges of simply supported panel

Considering the simply supported panel, subjected lifting force q_1 , the drag q_2 and axial compressive forces P_x and P_y . So the boundary conditions are:

$$w = N_{xy} = M_x = 0, N_x = -P_x h \text{ at } x = 0, a$$

$$w = N_{xy} = M_y = 0, N_y = -P_y h \text{ at } y = 0, b \quad (4.33)$$

The approximate solution of w and f satisfying the boundary condition (4.33) has the form [91]:

$$(w, w^*) = (W, \mu h) \sin \lambda_m x \sin \delta_n y \quad (4.34a)$$

$$f = A_1 \cos 2\lambda_m x + A_2 \cos 2\delta_n y + A_3 \sin \lambda_m x \sin \delta_n y + A_4 \cos \lambda_m x \cos \delta_n y - \frac{1}{2} P_x h y^2 - \frac{1}{2} P_y h x^2 \quad (4.34b)$$

$\lambda_m = m\pi/a$, $\delta_n = n\pi/b$, W : amplitude of deflection and μ : is an imperfect parameter.

Replace equation (4.34a, 4.34b) into equation (4.28) and apply the Galerkin method, we have the equation result:

$$\frac{ab}{4} \left[\begin{array}{l} P_1 \frac{(F_2 F_4 - F_1 F_3)}{F_2^2 - F_1^2} \lambda_m^4 + P_2 \frac{(F_2 F_4 - F_1 F_3)}{F_2^2 - F_1^2} \delta_n^4 + P_3 \frac{(F_2 F_4 - F_1 F_3)}{F_2^2 - F_1^2} \lambda_m^2 \delta_n^2 \\ - P_4 \frac{(F_2 F_3 - F_1 F_4)}{F_2^2 - F_1^2} - P_5 \frac{(F_2 F_3 - F_1 F_4)}{F_2^2 - F_1^2} + P_6 \lambda_m^4 + P_7 \delta_n^4 + P_8 \lambda_m^2 \delta_n^2 \\ - \frac{(F_2 F_4 - F_1 F_3) \lambda_m^2}{F_2^2 - F_1^2} \frac{\lambda_m^2}{R} - k_1 - k_2 (\lambda_m^2 + \delta_n^2) \end{array} \right] W$$

$$- \left[\frac{2}{3} \lambda_m \delta_n \left(P_1 \frac{1}{A_{22}^*} + P_2 \frac{1}{A_{11}^*} \right) - \frac{1}{6 R A_{22}^*} \frac{\delta_n}{\lambda_m} \right] W (W + 2\mu h) \quad (4.36)$$

$$- \frac{ab}{64} \left(\frac{1}{A_{22}^*} \delta_n^4 + \frac{1}{A_{11}^*} \lambda_m^4 \right) W (W + \mu h) (W + 2\mu h)$$

$$+ \frac{8(F_2 F_4 - F_1 F_3)}{3(F_2^2 - F_1^2)} \lambda_m \delta_n W (W + \mu h) + \frac{abh}{4} (P_x \lambda_m^2 + P_y \delta_n^2) (W + \mu h)$$

$$+ \frac{4(q_1 + q_2)}{\lambda_m \delta_n} - \frac{4h}{\lambda_m \delta_n} \frac{P_y}{R} = \frac{ab\rho_1}{4} \frac{\partial^2 W}{\partial t^2}$$

Where: m and n are odd numbers. (4.36) is the governing equation for the nonlinear dynamic response of a three-phase composite panel (all edges simply supported) subjected the impact of hydrodynamic loads.

From (4.36), the oscillation frequency of the perfect panel ($\mu = 0$) is determined as:

$$\omega_{mn} = \sqrt{-\frac{(b_1 + b_2)}{\rho_1}} \quad (4.37)$$

4.2.2. In case of four clamped edges

Considering the clamped edges panel, subjected lifting force q_1 , the drag q_2 and axial compressive forces P_x and P_y . So the boundary conditions are:

$$\begin{aligned} w = \partial w / \partial x = N_{xy} = 0, \quad N_x = -P_x h \quad \text{at } x = 0, a \\ w = \partial w / \partial y = N_{xy} = 0, \quad N_y = -P_y h \quad \text{at } y = 0, b \end{aligned} \quad (4.38)$$

The approximate solution of w and f satisfies the boundary condition (4.38) has the form:

$$(w, w^*) = (W, \mu h)(1 - \cos 2\lambda_m x)(1 - \cos 2\delta_n y) \quad (4.39a)$$

$$\begin{aligned} f = Q_1 \cos 2\lambda_m x + Q_2 \cos 2\delta_n y + Q_3 \cos 4\delta_n y + Q_4 \cos 2\lambda_m x \cos 2\delta_n y \\ + Q_5 \cos 2\lambda_m x \cos 4\delta_n y + Q_6 \cos 4\lambda_m x \cos 2\delta_n y \\ + Q_7 \cos 4\lambda_m x + Q_8 \sin 2\lambda_m x \sin 2\delta_n y - \frac{1}{2} P_x h y^2 - \frac{1}{2} P_y h x^2 \end{aligned} \quad (4.39b)$$

$\lambda_m = m\pi / a, \delta_n = n\pi / b, W$: amplitude of deflection and μ : is an imperfect parameter.

Replace equation (4.39a, 4.39b) into equation (4.28) and apply the Galerkin method, we have the equation result (Appendix E):

$$\begin{aligned} \rightarrow -ab \left[8\lambda_m^4 \frac{B_{21}^*}{A_{22}^*} P_1 + 4\lambda_m^4 \frac{(F_1 F_6 + F_2 F_4)}{F_1 - F_2} P_1 + 8\delta_n^4 \frac{B_{12}^*}{A_{11}^*} P_2 + 4\delta_n^4 \frac{(F_1 F_6 + F_2 F_4)}{F_1 - F_2} P_2 - \right. \\ \left. 4\lambda_m^2 \delta_n^2 P_3 - 12\lambda_m^4 P_6 - 12\delta_n^4 P_7 - 4\lambda_m^2 \delta_n^2 P_8 + 2.25k_1 + 3k_2 \lambda_m^2 + \right. \\ \left. 3k_2 \delta_n^2 \right] W - 4ab \lambda_m^2 \delta_n^2 \left[\frac{(\lambda_m^4 P_1 + \delta_n^4 P_2)}{F_1 - F_2} F_1 + \left(\frac{P_1}{A_{22}^*} + \frac{P_2}{A_{11}^*} \right) \right] W(W + 2\mu h) + \\ 8\lambda_m^2 \delta_n^2 \left[\frac{B_{12}^*}{A_{11}^*} + \frac{B_{21}^*}{A_{22}^*} + \frac{(F_1 F_6 + F_2 F_4)}{F_1 - F_2} \right] W(W + \mu h) - \frac{ab}{4} \left[17 \frac{\lambda_m^4}{A_{11}^*} + \right. \\ \left. \frac{16\lambda_m^4 \delta_n^4}{2\lambda_m^4 A_{22}^* + 8\lambda_m^2 \delta_n^2 E_1 + 32\delta_n^4 A_{11}^*} + 17 \frac{\delta_n^4}{A_{22}^*} + \frac{16\lambda_m^4 \delta_n^4}{32\lambda_m^4 A_{22}^* + 8\lambda_m^2 \delta_n^2 E_1 + 2\delta_n^4 A_{11}^*} - \right. \\ \left. \frac{32\lambda_m^4 \delta_n^4 F_1}{ab(F_1 - F_2)} \right] W(W + 2\mu h)(W + \mu h) + 3abh(\lambda_m^2 P_x + \delta_n^2 P_y)(W + \mu h) + \\ \left(q_1 + q_2 - \frac{P_y h}{R} \right) ab = ab \rho_1 \frac{\partial^2 W}{\partial t^2} \end{aligned} \quad (4.41)$$

Where: m and n are odd numbers. (4.41) is the governing equation for the nonlinear dynamic response of a three-phase composite panel (all edges clamped) subjected the impact of hydrodynamic loads.

From (4.41), the oscillation frequency of the perfect panel ($\mu = 0$) is determined as:

$$\omega_{mn} = \sqrt{-\frac{(b_1 + b_2)}{\rho_1}} \quad (4.42)$$

4.3. Testing the reliability of the calculation program.

The thesis's calculation program is built in a Matlab environment called

Buckling of Panel. The author has used this program to calculate and compare with the Ansys software and [27]. Input parameters: The panel size: $axbxt=1x0.31x0.02m$ (Figure 4.10); Order of layering: $[0/90/0/90/90/0/90/0]_5$ và $[90/0/45/-45/-45/45/0/90]_5$; $E_{11}=31.009(GPa)$, $E_{22}=E_{33}=6.016(GPa)$, $\nu_{12}=\nu_{13}=0.3$, $\nu_{23}=0.43$, $G_{12}=G_{13}=1.985(GPa)$, $G_{23}=1.966(GPa)$, load $P_0 = 387860(Pa)$

4.3.1. In case of orthotropic plates $[0/90/0/90/90/0/90/0]_5$

Table 4.8. The comparison result for the reliability testing of calculation program with the orthotropic plates

Case	Maximum deflection of panel W (m)			Difference (%) between (2) và (4)
	Buckling of Panel	Bertholot [27]	Ansys	
(1)	(2)	(3)	(4)	(5)
All edges simply supported	0.001222	0.001199	0.001244	1.77
All edges clamped	0.0002476	0.000272	0.000256	3.28

The difference between (2) and (4) is $1.77 \div 3.28\%$, Buckling of Panel is sufficiently reliable to calculate.

4.3.2. In case of layering plate $[90/0/45/-45/-45/45/0/90]_5$

Table 4.9 The comparison result with the layering plate $[90/0/45/-45/-45/45/0/90]_5$.

Case	Maximum deflection of panel W (m)		Difference (%) between (2) và (3)
	Buckling of Panel	Ansys	
(1)	(2)	(3)	(4)
All edges simply supported	0.001395	0.001372	1.65
All edges clamped	0.0003114	0.000319	2.38

The difference between (2) and (3) is $1.65 \div 2.38\%$, Buckling of Panel is sufficiently reliable to calculate.

4.4. Survey on effect of certain factors on buckling of three-phase composite panel subjected hydrodynamic load.

Lift wing is a complex structure with large loads, to ensure safety in this section will investigate the case of simply supported panel. Hydrofoils operate in waves under the conditions of foilborne, hydrodynamic load acting on the foil is expressed as [48]:

$$P = P_0 \sin(\omega t - kx) (N/m^2) \quad (4.43)$$

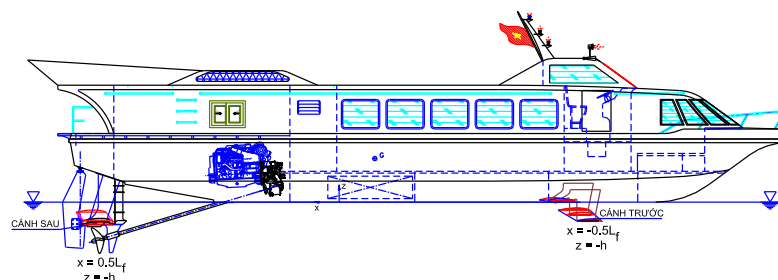


Figure 4.22. Hydrofoil ship with completely submerged foil have a geometric center at $(\pm 0.5L_f, 0, -h)$ as indicated with the hull and struts.

Survey of three-phase composite panel with dimensions $axbxt = 1.0x0.31x0.02m$, which is the cover of lift foil at the shape and dimensions as shown in

Figure 4.10 and Section 4.1.2.2, subjected the hydrodynamic load P (determined from the formula 4.43), the panel is made of the component materials: Epoxy matrix: $E_m=3.50 \text{ GP}_a$, $\nu_m=0.33$; Cimax fibers: $E_a=58.85 \text{ GP}_a$, $\nu_a=0.240$; TiO_2 particles: $E_c=5.58 \text{ GP}_a$, $\nu_c=0.20$. (4.44)

4.4.1. Effect of layer layout.

Figure 4.23 shows that the dynamic response of the three-phase composite panel in 03 cases of different layering and fiber direction significantly affects the buckling of the plate. Layer layout $[90/0/45/-45/-45/45/0/90]_5$ gives greater panel oscillation than other layer layouts.

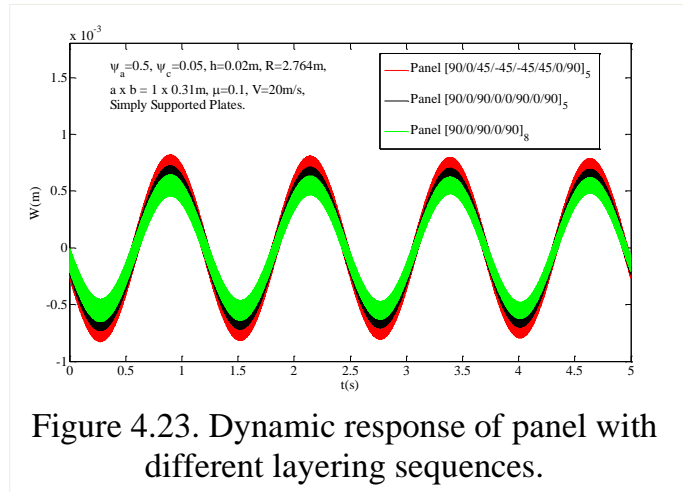


Plate of layer $[90/0/45/-45/-45/45/0/90]_5$ (Section 4.1.2.2) as

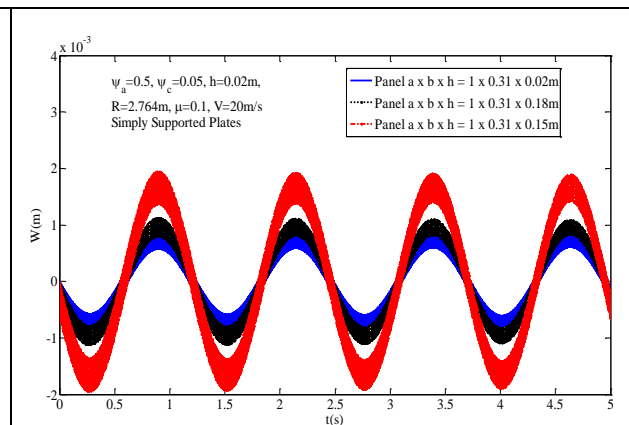
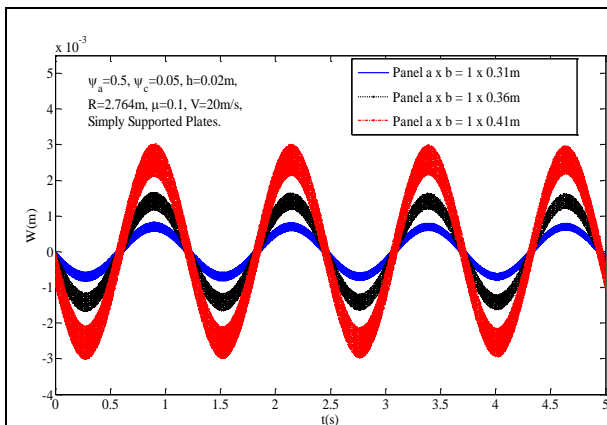
stable quasi-isotropic materials in all directions, combined with the results of the survey shows the stable panel, so this layer layout is selected to consider dynamic response for the next case.

4.4.2. Effect of panel geometry dimension.

Figures 4.24 and 4.25 illustrate the effect of width b ; thickness h on nonlinear dynamic response of three-phase composite panel. Panel deformation increases by the increase in width b and decrease in panel thickness. The distance between the stringers of the foil is $\leq 310\text{mm}$ when the foil structure is stable.

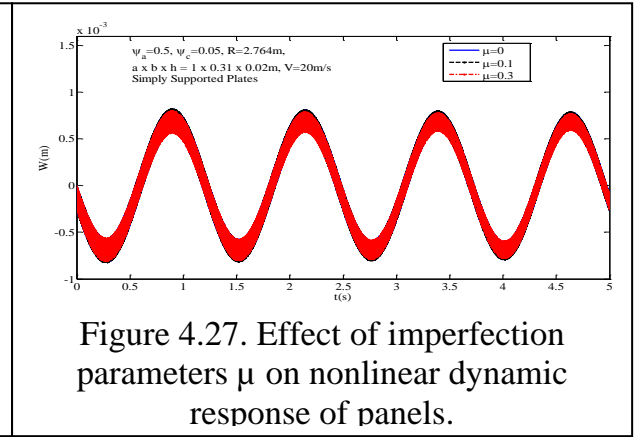
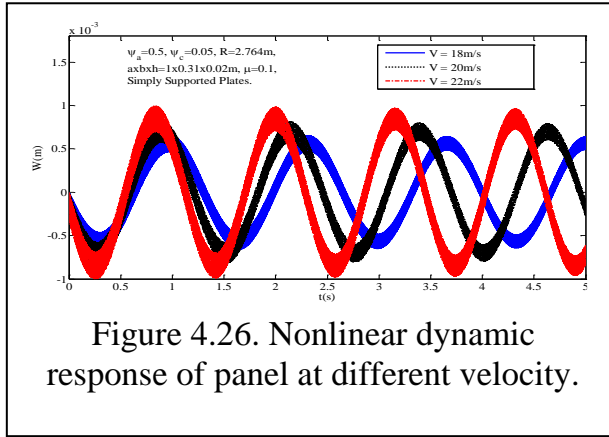
4.4.3. Effect of ship speed

Figure 4.26 shows the effect of ship speed on the nonlinear dynamic response of the three-phase composite panel. Panel deformation increases by the speed increase.

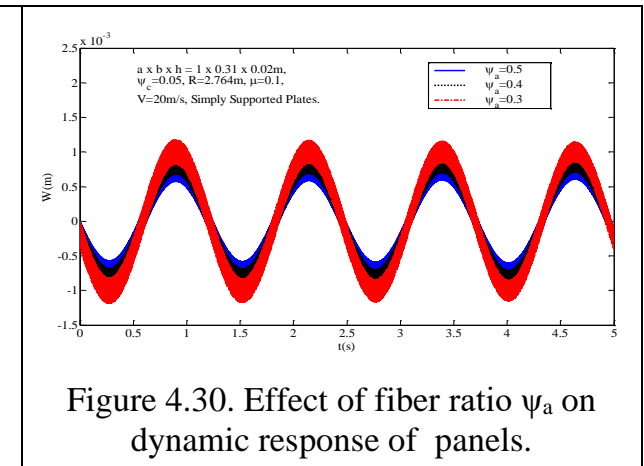
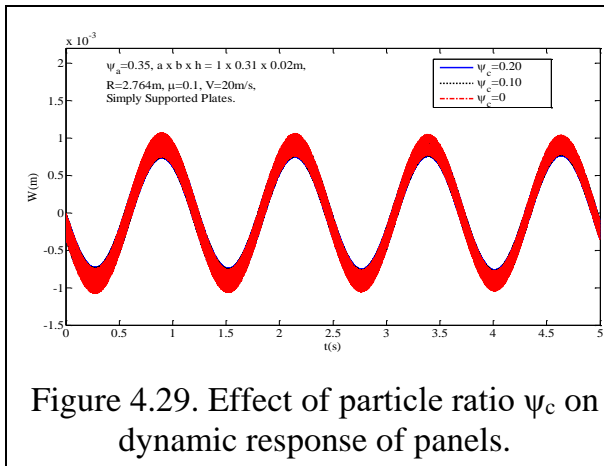


4.4.4. Effect of initial imperfection

Figure 4.27 show the effect of initial imperfection μ on dynamic response of three-phase composite panels. When μ increases in the range of $0 \div 0.1$, deformation of panels increases and when μ increases in the range of $0.1 \div 0.3$, deformation of panels decreases. Effect of parameter μ on panel deformation is small to neglectable.



4.4.5. Effect of three-phase composite material ratio.



Figures 4.29 and 4.30 show the effect of fiber and particle on the dynamic response of three-phase composite panels. It is obvious that an increase in fiber density will reduce the panel's amplitude of fluctuation and the more the density of the particle will reduce the panel's flexural strength. The effect of fiber is better than particle.

4.4.6. Effect of geometrical dimensions, fiber and particle ratio on oscillation frequency of three-phase composite panel.

Table 4.18. Effect factors on oscillation frequency of three-phase composite panel.

ψ_a	ψ_c	$\omega_{mn} \text{ (rad/s)}$					
		a = 1.0 m, b = 0.31 m			a = 1.0 m, b = 0.36 m		
		h=0.015m	h=0.018m	h=0.020m	h=0.015m	h=0.018m	h=0.020m
0.55	0	2.3375e3	2.8033e3	3.1139e3	1.7769e3	2.1283e3	2.3628e3
0.50	0.05	2.2570e3	2.7066e3	3.0065e3	1.7156e3	2.0549e3	2.2813e3
0.45	0.10	2.1744e3	2.6077e3	2.8966e3	1.6529e3	1.9797e3	2.1978e3
0.40	0.10	2.0842e3	2.4994e3	2.7763e3	1.5842e3	1.8974e3	2.1065e3

Table 4.18 shows that for foils whose is $b = 0.31\text{m}$ will have the oscillation frequency which is 1.32 times greater than in the case of $b = 0.36\text{m}$ (a decrease of 1.32 times in

the hardness level of foil).

4.4.7. Effect of foil distance.

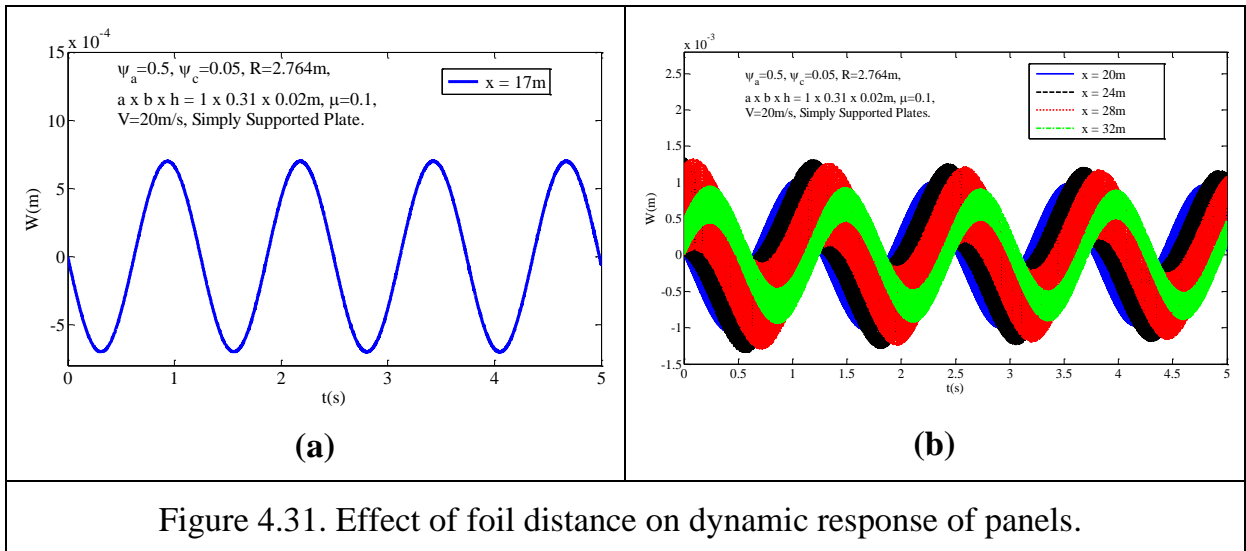


Figure 4.31. Effect of foil distance on dynamic response of panels.

It is shown in the figure 4.31 that: Foil deformation depends on distance of two foils and operating region of the ship which caused by the impact of wave resonance:

- + Deformation of foils will be largest when the foil position is $x = \lambda/4 + n\lambda/2$.
- + Foil deformation will be smallest when the foil position is $x = n\lambda/2$ (n : is an integer, positive).

4.6. Chapter 4 conclusion

- The function and regression curve of the allowable deflection of foil with chord length $c = 2 \div 7(\text{ft})$ is built as the basis for selecting a structure to ensure buckling.
- (4.36) and (4.41) are established as governing equations for the nonlinear dynamic response of three-phase composite panels subjected hydrodynamic load in two cases of all simply supported and clamped edges.
- (4.37) and (4.42) are established as expressions determining oscillation frequency of three-phase composite panels in two cases of all simply supported and clamped edges

CONCLUSIONS

- The equation and the static buckling calculation of the three-phase polymer orthotropic composite plates have been established, which are subject to one-direction compression, simultaneous compression in both directions and shear load.
- The equation and the dynamic buckling calculation of three-phase polymer composite panels with hydrodynamic load have been established in two cases of all simply-supported and clamped edges.
- Constructed method of buckling calculation of hydrofoil lift wings by analytical method based on design criteria of hydrofoil structure.
- Assess the influence of factors on the static and dynamic stability of three-phase composite plates. Therefore, it is possible to change these parameters to choose a reasonable design and actively control the behavior of the structure.

LIST OF PUBLISHED RESEARCH WORKS BY AUTHOR RELATED TO THE THESIS

1. **Pham Van Thu**, Tran Quoc Quan, Homayoun Hadavinia, Nguyen Dinh Duc (2014). Nonlinear dynamic analysis and vibration of imperfect three phase polymer nanocomposite panel resting on elastic foundation under hydrodynamic loads. Proceeding of The Third International Conference on Engineering Mechanics and Automation (ICEMA 2014), Hanoi, October- 2014, ISBN: 978-604-913-367-1, pp. 499-508.
2. **Pham Van Thu**, Nguyen Dinh Duc (2016). Nonlinear dynamic response and vibration of an imperfect three-phase laminated nanocomposite cylindrical panel resting on elastic foundations in thermal environments. *J. Science and Engineering of Composite Materials*, DOI: 10.1515/secm-2015-0467 (De Gruyter, SCIE, IF=0.593).
3. **Pham Van Thu**, Nguyen Dinh Duc (2016). Nonlinear stability analysis of imperfect three-phase sandwich laminated polymer nanocomposite panels resting on elastic foundations in thermal environments. *Journal of Science, Mathematics-Physics*, Vietnam National University, Hanoi, Vol.32, N1, pp 20-36.
4. **Pham Van Thu**, Trinh Van Binh, Huynh Tan Dat, Nguyen Van Dat, Nguyen Dinh Duc (2016). Study to determine computational stress for orthotropic plates used in composite shipbuilding. National Conference on Composite Materials and Structures, Mechanics, Technology and Applications, Nha Trang University, July 28-29, 2016, pages 675-682.
5. **Nguyen Dinh Duc**, Pham Van Thu (2014). Nonlinear stability analysis of imperfect three-phase polymer composite plates in thermal environments. *J. Composite Structures*, Vol.109, pp.130-138. (Elsevier, SCIE, IF=3.12).
6. **Nguyen Dinh Duc**, Homayoun Hadavinia, Pham Van Thu, Tran Quoc Quan (2015). Vibration and nonlinear dynamic response of imperfect three-phase polymer nanocomposite panel resting on elastic foundations under hydrodynamic loads. *J. Composite Structures*, Vol.131, pp.229-237 (Elsevier, SCIE, IF=3.12).
7. **Pham Van Thu**, (2018). The buckling of orthotropic three-phase composite plates used in composite shipbuilding. *Journal of Science, Mathematics- Physics*, Vietnam National University, Hanoi, Vol.34, N4, pp 92-109.